

**Search for WIMP Annual Modulation Signature:
Results from DAMA/NaI-3 and DAMA/NaI-4
and the Global Combined Analysis**

DAMA Collaboration

also ROM2F/2000/01 (January 2000) and submitted for publication

INFN – Laboratori Nazionali del Gran Sasso

Search for WIMP annual modulation signature: results from DAMA/NaI-3 and DAMA/NaI-4 and the global combined analysis

R. Bernabei^a, P. Belli^a, R. Cerulli^a, F. Montecchia^a, M. Amato^b, G. Ignesti^b, A. Incicchitti^b, D. Prospero^b, C.J. Dai^c, H.L. He^c, H.H. Kuang^c, J.M. Ma^c

^a *Dip. di Fisica, Universita' di Roma "Tor Vergata" and INFN, sez. Roma2, I-00133 Rome, Italy*

^b *Dip. di Fisica, Universita' di Roma "La Sapienza" and INFN, sez. Roma, I-00185 Rome, Italy*

^c *IHEP, Chinese Academy, P.O. Box 918/3, Beijing 100039, China*

Abstract

The data, collected by the $\simeq 100$ kg NaI(Tl) DAMA set-up at the Gran Sasso National Laboratory of I.N.F.N. during two further yearly cycles (DAMA/NaI-3 and DAMA/NaI-4; statistics of 38475 kg·day), have been analysed in terms of WIMP annual modulation signature. The results agree with those previously achieved. The cumulative analysis of all the available data (DAMA/NaI-1 to 4; statistics of 57986 kg·day) favours the possible presence of a WIMP with $M_w = (52_{-8}^{+10})$ GeV and $\xi\sigma_p = (7.2_{-0.9}^{+0.4}) \cdot 10^{-6}$ pb at 4σ C.L., when standard astrophysical assumptions are considered. The allowed mass extends up to 105 GeV (1σ) when the uncertainty on the mean value of the local velocity v_0 is taken into account and up to 132 GeV (1σ) in case a possible bulk halo rotation is also considered. Moreover, the allowed regions extend to lower $\xi\sigma_p$ values when the limit achieved in DAMA/NaI-0 is included in the cumulative analysis (favouring e.g., in case of standard assumptions, $M_w = (44_{-9}^{+12})$ GeV and $\xi\sigma_p = (5.4 \pm 1.0) \cdot 10^{-6}$ pb at $\simeq 4 \sigma$ C.L.). The regions in the $\xi\sigma_p$ versus M_w plane allowed for the possible signal at 3σ C.L. are given.

1 INTRODUCTION

The $\simeq 100$ kg NaI(Tl) DAMA set-up is running at the Gran Sasso National Laboratory of I.N.F.N. [1, 2, 3, 4, 5, 6, 7, 8, 9, 10, 11]; its main goal is to search for Weakly Interacting Massive Particles (WIMPs). According to the standard description, these particles would have in the galactic halo a Maxwellian velocity distribution with a cut-off at the galactic escape velocity; therefore, a WIMP "wind" would continuously hit the Earth. The WIMPs can be detected by investigating their elastic scattering on the target nuclei of a detector. The nuclear recoil energy in the keV range is the measured quantity. The best signature to single out the possible presence of a WIMP signal from the background is the so-called *annual modulation signature* [4, 5, 6, 12, 13]. In fact, since the Earth rotates around the Sun, it would be crossed by a larger WIMP flux in June (when its rotational velocity is summed to the one of the solar system with respect to the Galaxy) and by a smaller one in December (when the two velocities are subtracted), inducing a peculiar modulation of the low energy rate [4, 5, 6, 12, 13]. A WIMP induced effect would exhibit all the following requirements: i) modulation of the "single hit" rate ¹; ii) only in a defined low energy region; iii) according to a cosine function; iv) with proper period T (1 year); v) with proper phase t_0 ($\simeq 2$ June, that is about the 152.5th day in the year); vi) with proper modulated amplitude ($\lesssim 7\%$ in the region of maximal sensitivity).

At present the lightest supersymmetric particle named neutralino, whose interaction with ordinary matter is mainly spin-independent (SI), is considered the best candidate for WIMP; in the following we will devote particular attention to this case (see sects. 4 and 5).

Investigations exploiting statistics of 4549 kg·day (DAMA/NaI-1) and of 14962 kg·day (DAMA/NaI-2) have been already presented in refs. [4, 5, 6], while the possible implications have been discussed in refs. [14, 15, 16].

The detailed description of the DAMA set up and its performances have been presented in ref. [1], where the radiopurity of all its components has also been discussed. Moreover, in refs. [6, 17, 18] some specific considerations on the realization of radiopure NaI(Tl) detectors have been addressed. The data were collected with nine 9.70 kg NaI(Tl) crystal scintillators in suitably radiopure Cu housings. Each detector has two 10 cm long tetrasil-B light guides directly coupled to the opposite sides of the bare crystal. Two low background photomultipliers work in coincidence and collect light at single photoelectron threshold; 2 keV is the used software energy threshold [1, 2, 4, 5, 6, 11]. The detectors are housed in a low radioactive sealed copper box inside a low radioactivity multicomponent shield (paraffin/polyethylene/Cd foils/Pb/Cu) from environmental background. A high purity (HP) Nitrogen atmosphere – in slightly overpressure with respect to the external environment – is maintained inside the copper box by a continuous flux of HP Nitrogen gas from bottles stored underground since time. The whole shield is also sealed and maintained in HP Nitrogen atmosphere; particular care was also devoted to obtain

¹When searching for WIMPs with a multi-detector set-up (as DAMA/NaI), the low energy rates are always referred to events where only one detector is firing ("single hit" events), being negligible the probability that a WIMP will interact in more than one.

an experimental site as much air-tight as possible. The installation is subjected to air conditioning to avoid any significative influence of the temperature (see refs. [1, 4, 5, 6] and later).

2 DAMA/NaI-3 AND DAMA/NaI-4 DATA SETS AND THE STABILITY CONTROLS

The DAMA/NaI-3 data were collected roughly from middle August 1997 to the end of September 1998 (22455 kg·day statistics), while DAMA/NaI-4 refers to data collected roughly from middle October 1998 until the second half of August 1999 (16020 kg·day statistics)².

The typical differential counting rate in the region between 2 and 20 keV has been previously reported in refs. [4, 5, 8], while the one between $\simeq 1$ and 10 keV cumulatively has been reported³ in ref. [11]; the shapes of the energy distribution of each detector are quite similar. Moreover, in ref. [9] higher energy parts of the cumulative energy spectrum have also been presented. For completeness, fig. 1 shows the cumulative energy spectrum near the used 2 keV software energy threshold for the data of the two yearly cycles considered here.

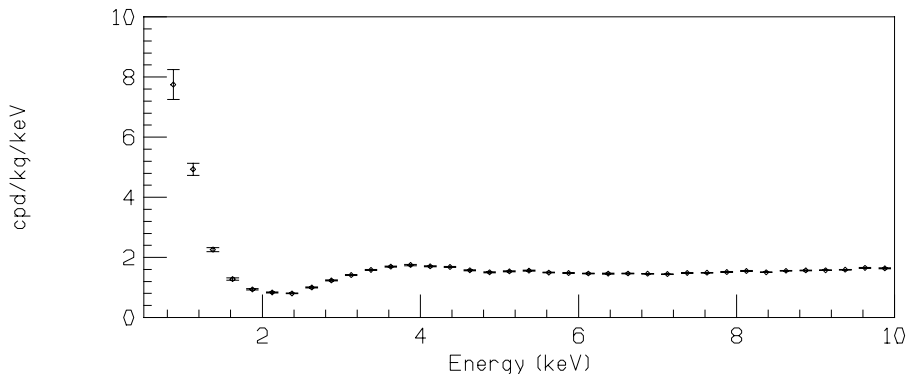


Figure 1: Cumulative energy spectrum near the used 2 keV software energy threshold (DAMA/NaI-3 and DAMA/NaI-4 data). This distribution refers – as usual in our experiment – to ”single hit” events (that is each detector has all the others as veto).

We recall that the rejection of residual noise near energy threshold is performed exploiting the distributions — different for scintillation pulses (signals with decay times of

²Some upgradings have been performed before the DAMA/NaI-4 running period.

³This is the region of maximal interest to search for SI coupled WIMPs because of: i) the quasi-exponential energy distribution of the induced nuclear recoils; ii) the possible annual modulation effect singled out in the lowest energy bins in refs. [4, 5, 6]; iii) the location of the first pole of the Iodine form factor [19]. Note that the software energy threshold has been so far cautiously taken at 2 keV to assure a full noise rejection near it with the used strategy[1].

order of hundreds ns) and noise pulses (PMT fast signals with decay times of order of tens ns) — of several variables built by using the information recorded over 3250 ns by a Lecroy Transient Digitizer [1, 2, 4, 5]; examples of these distributions as well as the evaluation of the corresponding software cut efficiencies can be found in ref. [1].

The stability of the efficiencies over the whole data taking periods has been investigated; their percentage variations e.g. in the (2-8) keV energy interval show a gaussian distribution with $\sigma = 0.6\%$ and 0.5% for DAMA/NaI-3 and DAMA/NaI-4, respectively. Moreover, the time behaviour of these percentage variations does not show any modulation with the period and phase expected for a WIMP signal. In particular, in the (2-4) keV energy interval a modulated amplitude (considering the two periods all together) equal to $(1.0 \pm 1.0) \cdot 10^{-3}$ is found, while in the (4-6) keV it results $(0.1 \pm 0.7) \cdot 10^{-3}$, both evidently consistent with zero. Similar results are obtained in other energy bins.

In long term running conditions, the knowledge of the energy scale is assured by periodical calibration with ^{241}Am source and by continuously monitoring in the same production data (summing them each $\simeq 7$ days) the position and resolution of the ^{210}Pb peak⁴ (46.5 keV) [1, 4, 5]. As in refs. [5, 6], the distribution of the relative variations of the energy calibration factors, estimated from the position of this peak for all the 9 detectors during both DAMA/NaI-3 and DAMA/NaI-4 without applying any correction, has been investigated; it shows a gaussian behaviour with $\sigma = (0.95 \pm 0.04)\%$. Considering that the results of the routine calibrations are obviously properly taken into account in the data analysis, such a result allows to conclude that the energy calibration factors for each detector are known with an uncertainty $< 1\%$. Due to the relatively poor energy resolution of the detectors at low energy, this could give rise only to an additional relative energy spread $\lesssim 10^{-4}$ in the lowest energy region and $\lesssim 10^{-3}$ at 20 keV, which is negligible.

All the relevant stability parameters have been quantitatively investigated for each data set, obtaining time behaviours like the ones shown in refs. [4, 5, 6]. In particular, as already discussed in refs. [1, 5, 6], the observed variations of the temperature can only induce a practically negligible variation of the light output, in agreement with the results obtained by the long term routine and intrinsic calibrations [1, 4, 5]. Further, as already discussed in refs. [1, 4, 5, 6], the detectors are *excluded* from environmental Radon being housed in a sealed Cu box which is continuously flushed with a large flux of high purity (HP) N_2 and maintained in a slight overpressure with respect to the environment [1, 4, 5] (see also sect. 1). In addition, the observed time behaviour of the external Radon level allows to exclude the presence in it of a cosine modulated component with the period and phase expected for a WIMP signal; in fact, a fit gives for its amplitude the values $(0.14 \pm 0.25) \text{ Bq/m}^3$ during DAMA/NaI-3 and $(0.12 \pm 0.20) \text{ Bq/m}^3$ during DAMA/NaI-4, evidently consistent with zero.

The distribution of the total hardware rate of the nine detectors (R_H) above the single photoelectron threshold (i.e. from noise to "infinity") has also been investigated; it shows a gaussian behaviour with $\sigma = 0.6\%$ for DAMA/NaI-3 and $\sigma = 0.4\%$ for DAMA/NaI-4,

⁴It is present at level of few cpd/kg in the measured energy distributions, mainly because of a surface contamination by environmental Radon occurred during the first period of the detectors storage underground.

values which are in agreement with those expected on the basis of statistical arguments. Furthermore, no evidence for time modulation of R_H has been found.

The measured energy distributions in energy regions not involved in the Dark Matter direct detection for DAMA/NaI-3 and DAMA/NaI-4 have been investigated as a function of the time in order to exclude that a modulation detected in the lowest energy region could be ascribed to a background modulation⁵. For this purpose, according to refs. [5, 6], we have investigated the rate integrated from 90 keV to "infinity", R_{90} , as a function of the time. The distributions of the percentage variations of R_{90} with respect to their mean values for all the crystals during both DAMA/NaI-3 and DAMA/NaI-4 show a gaussian behaviour with $\sigma \simeq 1.3\%$ and $\sigma \simeq 1.0\%$, respectively, values well accounted by the expected statistical spread. Moreover, fitting the behaviour of R_{90} with time, adding also a term modulated according to a cosine function with 1 year period and 152.5 day phase (as expected for a WIMP signal), the value (-0.11 ± 0.33) cpd/kg has been found for the modulated amplitude in the DAMA/NaI-3 data and (-0.35 ± 0.32) cpd/kg in the DAMA/NaI-4 ones, clearly consistent with zero. These results allow to exclude the presence of a background modulation in the whole energy spectrum at a level much lower than the possible signal modulation found in the lowest energy region (see refs. [4, 5] and later); in fact, otherwise, the modulated amplitude for R_{90} should be of order of tens cpd/kg, that is $\simeq 100$ standard deviations far away from the measured value. Finally, focusing the attention on an energy region nearer to the one where the possible signal is present [4, 5], e.g. 10-20 keV, the values (-0.0044 ± 0.0044) cpd/kg/keV and (-0.0071 ± 0.0044) cpd/kg/keV are found for the modulated amplitude in DAMA/NaI-3 and in DAMA/NaI-4, respectively; they can be considered statistically consistent with zero.

The quantitative investigations reported in this section offer a complete analysis of the possible sources of systematic effects, which could affect the energy spectrum. These investigations credit a percentage systematic error $\lesssim 10^{-3}$ on the basis of the measured variations of temperature, calibration uncertainties, etc. Moreover, the results on the analysis of R_{90} exclude even at more stringent level the presence of an overall background modulation (excluding also significant contribution e.g. from possible surviving neutrons from the environment). Finally, no contribution can arise from environmental Radon being the detectors excluded from it (in addition, a time correlation analysis offers, as mentioned, a Radon modulated contribution compatible with zero).

We want to point out here that really the systematic effects of interest are those able to satisfy the same six requirements as a WIMP induced effect (see sect. 1); no one has been found so far. The same features should be also satisfied by possible concurrent physical processes; the only one we found up to now: the muon modulation reported in ref. [20], would fail some of them, would yield a modulation in R_{90} (which is not observed) and

⁵In fact, the background in the lowest energy region is expected to be essentially due to Compton electrons, X-rays and/or Auger electrons, muon induced events, etc., which are strictly correlated with the events in the higher energy part of the spectrum; therefore, if a detected modulation with time in the lowest energy region would be due to a background modulation (instead of a possible signal), an equal or higher (sometimes much higher) modulation in the highest energy region should also be present.

– in any case – would offer in our set-up modulated amplitudes $\ll 10^{-4}$ cpd/kg/keV, much lower than we observe. So it can be discarded.

In conclusion, the results presented in this section allow to perform a statistical analysis of the data.

3 MODEL INDEPENDENT APPROACH: A VISUAL AID

As mentioned, the results discussed in the previous section allow to investigate the events in the lowest energy part of the energy spectrum in terms of WIMP annual modulation signature. A complete analysis [4, 5] will be carried out in the following sections, properly taking into account the energy and time differential distribution of the events. Here, in order to offer an immediate evidence of the presence of modulation in the lowest energy region of the experimental data, we show as an example in fig. 2 the model independent residual rate for the cumulative 2–6 keV energy interval as a function of the time along the years for all the available data (DAMA/NaI-1 to DAMA/NaI-4)⁶. Each data point has been obtained from the raw rate once subtracting the constant part (the weighted mean of the residuals must obviously be zero over the period), namely it is $\langle r_{ijk} - flat_{jk} \rangle_{jk}$. There the average is made on all the detectors (j index) and on all the 1 keV bins (k index) which constitute the considered energy interval; moreover, r_{ijk} is the rate in the considered i -th time interval for the j -th detector in the k -th energy bin, while $flat_{jk}$ is the rate of the j -th detector in the k -th energy bin averaged over the cycles.

The χ^2 test applied to the data of fig. 2 disfavors the hypothesis of unmodulated behaviour giving a probability of $4 \cdot 10^{-4}$ ($\chi^2/d.o.f. = 48/20$). On the other hand, fitting these residuals with the function $A \cdot \cos[\omega \cdot (t - t_0)]$ (obviously integrated in each of the considered time bin), one gets $A = (0.022 \pm 0.005)$ cpd/kg/keV, $T = \frac{2\pi}{\omega} = (1.00 \pm 0.01)$ year when fixing t_0 at 152.5 days and $A = (0.023 \pm 0.005)$ cpd/kg/keV, $t_0 = (144 \pm 13)$ days when fixing T at 1 year. In both cases $\chi^2/d.o.f. \simeq 23/18$. Similar results, but with larger errors, are found in case all the three parameters are kept free. As it is evident the period and the phase fully agree with the ones expected for a WIMP induced effect.

Let us now investigate the data with the complete needed sensitivity for WIMP mass and cross-section determination. At the end of sect. 5 we will come back to further comment on this approach, still using this particular 2–6 keV cumulative interval as an example.

⁶The bins considered in this figure for DAMA/NaI-3 and DAMA/NaI-4 are similar to those previously used for DAMA/NaI-1 and DAMA/NaI-2. We have verified that the results of this approach are substantially unchanged choosing other bins for this presentation. Moreover, we further stress that this presentation is only a visual aid, being the final results obtained by the full correlation analysis in time (1 day bin) and energy (1 keV bin) carried out in the following sections.

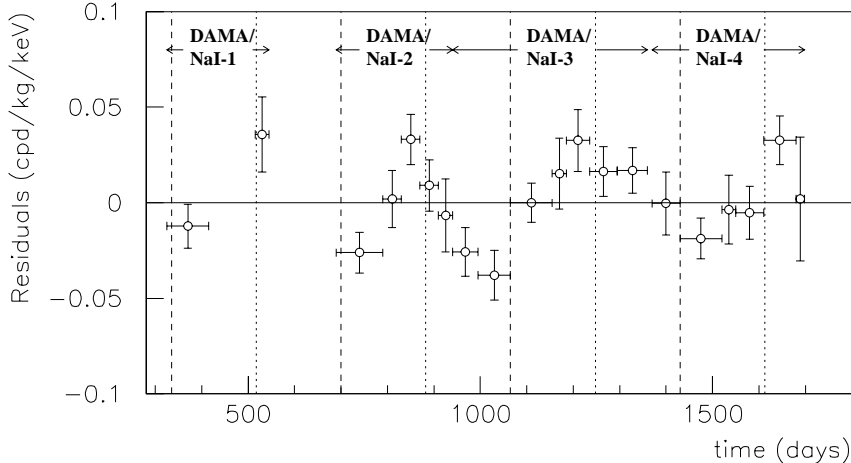


Figure 2: Model independent residual rate in the particular 2-6 keV cumulative energy interval as a function of the time elapsed since January 1-st of the first year of data taking. The expected behaviour of a WIMP signal is a cosine function with minimum roughly at the dashed vertical lines and with maximum roughly at the dotted ones.

4 FULL CORRELATION ANALYSIS OF THE DAMA/NaI-3 and DAMA/NaI-4 DATA SETS

According to refs. [4, 5], a complete time and energy correlation analysis of the data collected between 2 and 20 keV has been performed by using the standard maximum likelihood method. For this purpose the data have been grouped in cells identified by three indexes: i for the time interval (1 day each one), k for the energy bin ($\Delta E = 1$ keV each one) and j for the considered detector. The maximum likelihood function can be written as $\mathbf{L} = \prod_{ijk} e^{-\mu_{ijk}} \frac{N_{ijk}^{\mu_{ijk}}}{N_{ijk}!}$. Here N_{ijk} is the number of events in each ijk cell which follows a poissonian statistics with expected value equal to $\mu_{ijk} = [b_{jk} + S_{0,k} + S_{m,k} \cdot \cos\omega(t_i - t_0)] M_j \Delta t_i \Delta E \epsilon_{jk}$. The unmodulated and modulated parts of the signal are $S_{0,k}$ and $S_{m,k} \cos\omega(t_i - t_0)$, respectively; b_{jk} is the background contribution; Δt_i is the detector running time during the i -th day ($\Delta t \leq 1$ day); ϵ_{jk} are the overall efficiencies [1] and M_j is the detector mass.

Furthermore, pointing out the $S_{0,k}$ and $S_{m,k}$ dependence on M_w (the WIMP mass) and $\xi\sigma_p$ ($\xi = \frac{\rho_{WIMP}}{0.3\text{GeVcm}^{-3}}$ and σ_p WIMP scalar cross section on proton) by the expressions $S_{0,k} = \xi\sigma_p S'_{0,k}(M_w)$ and $S_{m,k} = \xi\sigma_p S'_{m,k}(M_w)$, we have: $\mathbf{L} = \mathbf{L}(N; b, M_w, \xi\sigma_p)$, where N is the set of all the N_{ijk} and b the set of all the b_{jk} . The maximum likelihood estimations of the free parameters b, M_w and $\xi\sigma_p$ are those values for which \mathbf{L} has its maximum for the given set of observations N , that is, those which minimize the function: $y = -2\ln(\mathbf{L}) - \text{const}$, with const chosen in order to have $y(\sigma_p=0)=0$ [4, 5]. The constraints

imposed in the minimization procedure [4, 5] are: $b_{jk} \geq 0$ and $M_w \geq 30$ GeV; the latter condition accounts for the more recent results achieved at accelerators on the neutralino mass. In the minimization procedure the WIMP mass has been varied up to 10 TeV.

As usual in particle Dark Matter direct searches [21], standard hypotheses have been used in the calculations of refs. [4, 5] for the distribution of astrophysical velocities, while a detailed investigation of the effects induced by their uncertainties [22] has been performed in ref. [7]. In this last reference it was shown that the uncertainties on the expected local velocity v_0 , as well as a possible bulk halo rotation, can play a significant role. In the following, for simplicity, the analysis of a single set (DAMA/NaI-3 or DAMA/NaI-4) will be performed by considering the standard value $v_0 = 220$ km/s, while the uncertainty on v_0 will be considered in the global analysis of all the available data for annual modulation analysis (DAMA/NaI-1 to 4).

By assuming the same standard astrophysical, nuclear and particle physics hypotheses employed in refs. [2, 4, 5], the minimum value of the y function is obtained for the DAMA/NaI-3 data when $M_w = (56_{-26}^{+18})$ GeV, $\xi\sigma_p = (9.7_{-3.5}^{+0.3})10^{-6}$ pb and, for the DAMA/NaI-4 data, when $M_w = (44_{-14}^{+32})$ GeV, $\xi\sigma_p = (6.9_{-3.8}^{+3.9})10^{-6}$ pb.

The goodness of the null hypothesis (absence of modulation) with respect to the hypothesis of presence of modulation with the obtained M_w and $\xi\sigma_p$ values has been tested for both periods by the maximum likelihood ratio [4, 5], obtaining that it favours the hypothesis of presence of modulation with the given M_w and $\xi\sigma_p$ at 98.3% C.L. for the DAMA/NaI-3 data and at 92.8% C.L. for the DAMA/NaI-4 data. Moreover, the goodness of the hypothesis of presence of modulation with the obtained M_w and $\xi\sigma_p$ has been even verified, according to ref. [23], by building the variable $z = \frac{1}{N} \cdot \sum_{ijk} [2(\mu_{ijk} - N_{ijk}) + 2N_{ijk} \ln(\frac{N_{ijk}}{\mu_{ijk}})]$ where N is the number of considered ijk cells. From the experimental data z comes out to be respectively 1.036 for DAMA/NaI-3 and 1.009 for the DAMA/NaI-4. The MonteCarlo distribution of z , evaluated as in ref. [5], gives a 19% probability to get a z value worse than 1.036 for DAMA/NaI-3 and 99.8% probability to get a z value worse than 1.009 for DAMA/NaI-4. Moreover, the z-test applied to the data of each detector shows that the data of all the detectors support the modulation at 95% C.L. in both data sets. Alternative analyses such as e.g. the one based on the χ_{test} variable described in ref. [5] offer substantially the same results.

In fig. 3 the regions allowed at 90% C.L. - for a SI coupled candidate - by the $\xi\sigma_p$ and M_w values obtained under standard assumptions by analysing the DAMA/NaI-3 (c) and DAMA/NaI-4 (d) data are shown superimposed to the ones credited by DAMA/NaI-1 (a) and DAMA/NaI-2 (b) [4, 5]. The limit curve at 90% C.L. achieved in ref. [2] (DAMA/NaI-0) is also reported. We take this occasion to recall that the DAMA/NaI-0 data are partially overlapped to the DAMA/NaI-1 data and have been analysed in ref. [2] in terms of pulse shape discrimination.

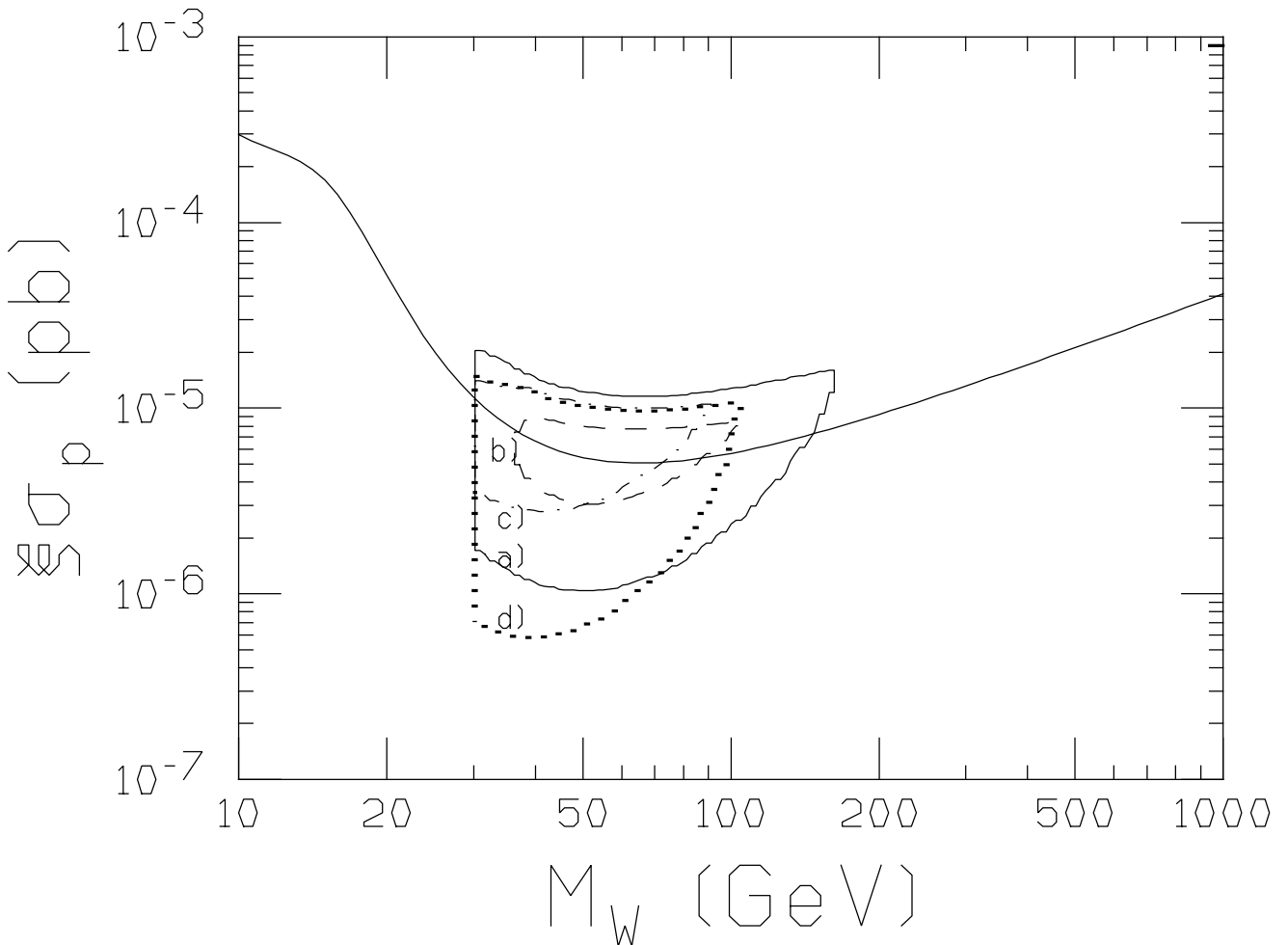


Figure 3: Regions allowed at 90% C.L. - for a SI coupled candidate - by the $\xi\sigma_p$ and M_w values obtained for DAMA/NaI-3 (c) and for DAMA/NaI-4 (d) data superimposed to the ones credited by DAMA/NaI-1 (a) and DAMA/NaI-2 (b) [4, 5]. The calculations have been performed according to the same astrophysical, nuclear and particle physics considerations as in refs. [4, 5]; in particular - as usual in particle Dark matter direct searches [21] - here the standard value $v_0 = 220$ km/s has been used. The limit curve at 90% C.L. achieved in ref. [2] (DAMA/NaI-0) is also shown.

5 FULL CORRELATION ANALYSIS OF ALL THE AVAILABLE DATA SETS

At this point we have analysed with the standard maximum likelihood method the available data all together. They refer to four different yearly cycles (DAMA/NaI-1 to DAMA/NaI-4) and the total statistics is 57986 kg·day.

Using the same strategy (and, in particular, $v_0 = 220$ km/s) as in the previous section and in refs. [4, 5], the minimum value of the y function is found for $M_w = (52_{-8}^{+10})$ GeV and $\xi\sigma_p = (7.2_{-0.9}^{+0.4})10^{-6}$ pb. The maximum likelihood ratio favours the hypothesis of presence of modulation with the given M_w and $\xi\sigma_p$ at 4 σ C.L.. The $S_{0,k}$ and $S_{m,k}$ values obtained by using the above quoted results of the maximum likelihood method are shown up to 6 keV in table 1 (above this energy S_m values are negligible). Performing the same analysis by the Feldman and Cousins approach [24], similar results are obtained.

Table 1: $S_{0,k}$ and $S_{m,k}$ values in the region of maximum interest for the possible signal as obtained by using the results of the global analysis for DAMA/NaI-1 to DAMA/NaI-4 with $v_0 = 220$ km/s and including or not the constraint arising from the results of DAMA/NaI-0 [2] (see text).

Energy (keV)	without constraint from DAMA/NaI-0		with constraint from DAMA/NaI-0	
	$S_{0,k}$ (cpd/kg/keV)	$S_{m,k}$ (cpd/kg/keV)	$S_{0,k}$ (cpd/kg/keV)	$S_{m,k}$ (cpd/kg/keV)
2-3	0.54 ± 0.09	0.023 ± 0.006	0.36 ± 0.10	0.021 ± 0.005
3-4	0.21 ± 0.05	0.013 ± 0.002	0.12 ± 0.05	0.010 ± 0.002
4-5	0.08 ± 0.02	0.007 ± 0.001	0.04 ± 0.02	0.004 ± 0.001
5-6	0.03 ± 0.01	0.003 ± 0.001	0.02 ± 0.01	0.002 ± 0.001

As in refs. [7, 18], the minimization procedure has been repeated by varying v_0 from 170 km/s to 270 km/s [22] to account for its present uncertainty and, also, including possible bulk halo rotation.

In fig. 4a) the regions allowed at 3 σ C.L. when: i) $v_0 = 220$ km/s (dotted contour); ii) v_0 uncertainty is taken into account (continuous contour); iii) possible bulk halo rotation is also considered (dashed contour), are shown. They are well embedded in the Minimal Supersymmetric Standard Model (MSSM) estimates for the neutralino [14].

To completely account for all our results on WIMP search, we have repeated the minimization procedure including the constraint arising from the exclusion plot given in ref. [2] (DAMA/NaI-0). It has been taken into account adding to the y function, defined above, a term: $\frac{(S_{0,k}-r_k)^2}{\sigma_k^2} \cdot \theta(S_{0,k} - r_k)$ where r_k and σ_k are the lowest counting rate and the associated error in the most selective energy bin of the data in ref. [2]. The Heaviside θ

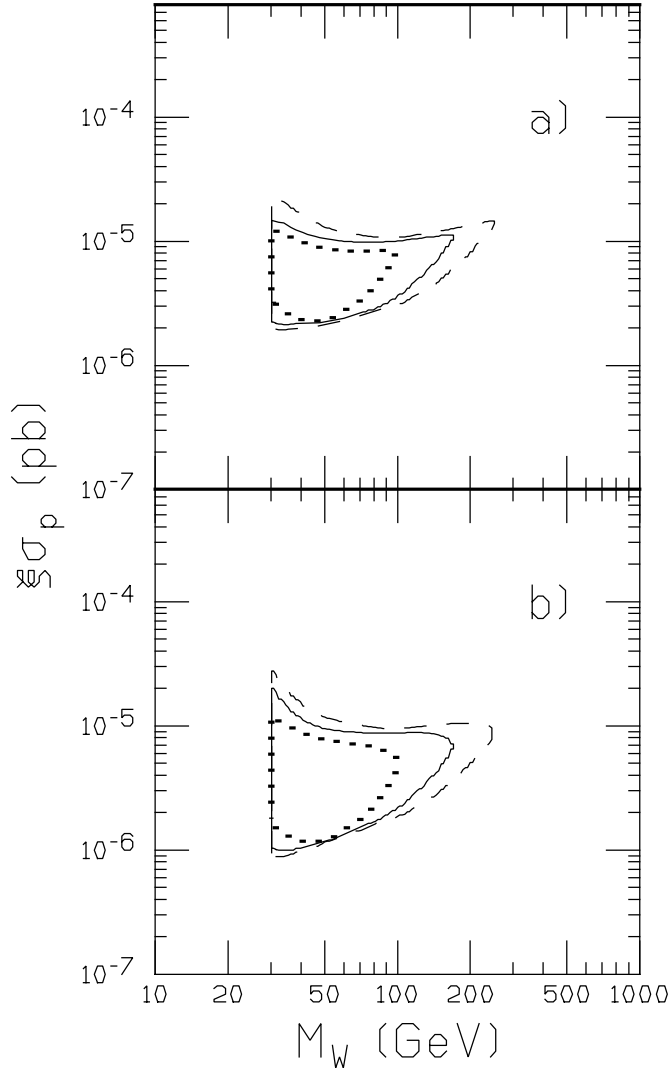


Figure 4: a) Regions allowed at 3σ C.L.: i) for $v_0 = 220$ km/s (dotted contour); ii) when accounting for v_0 uncertainty ($170 \text{ km/s} \leq v_0 \leq 270 \text{ km/s}$; continuous contour); iii) when considering also a possible bulk halo rotation as in ref. [7] (dashed contour); b) Regions allowed at 3σ C.L. – for the same conditions as previously reported – when including the constraint arising from the results of ref. [2].

function assures that this term contributes only when the expected value for $S_{0,k}$ is larger than r_k . In this way the minimum value of the y function – when $v_0 = 220$ km/s – is found for $M_w = (44_{-9}^{+12})$ GeV and $\xi\sigma_p = (5.4 \pm 1.0) \cdot 10^{-6}$ pb. The maximum likelihood ratio favours the hypothesis of presence of modulation with these M_w and $\xi\sigma_p$ at $\simeq 4\sigma$ C.L.; the corresponding $S_{0,k}$ and $S_{m,k}$ values can be found in table 1.

In fig. 4b) the regions allowed in this case at 3σ C.L. when: i) $v_0 = 220$ km/s (dotted contour); ii) v_0 uncertainty is taken into account (continuous contour); iii) possible bulk halo rotation is also considered (dashed contour), are shown.

Finally, to clearly show the relevance of performing a full correlation analysis (as the standard maximum likelihood considered above) able to properly account for all the features of the time and energy differential distribution of the measured events, we come back to the simple approach of sect. 3 where the particular cumulative 2–6 keV energy interval has been shown as an example. For this purpose, in table 2 we report the $\chi^2/d.o.f$ and the relative probabilities obtained by comparing the residuals of fig. 2 with the values expected when considering the M_w and $\xi\sigma_p$ values of the minima obtained by the cumulative analysis under standard assumptions, either considering (b) or not (a) the constraint from DAMA/NaI-0. As one can see in these cases, a good agreement for DAMA/NaI-1, DAMA/NaI-2 and DAMA/NaI-4 is found, while the agreement is poorer for DAMA/NaI-3. This is due to the first two DAMA/NaI-3 points in fig. 2, as shown by the $\chi^2/d.o.f$. (and probability value) obtained without them. Moreover, their fluctuation results significant only in one of the involved energy bins (obviously in statistics the tails can also play some role); in fact, if e.g. the residuals in the cumulative 2–5 keV energy interval (where most of the signal is expected) are indeed considered, the $\chi^2/d.o.f$. values (when taking into account all the residuals over the four yearly cycles) result 11.5/20 (93% probability) and 12.3/20 (91% probability), respectively.

At this point, we want to comment that, as for the case of v_0 and possible bulk rotation, some uncertainties can also arise from the standard nuclear and particle physics assumptions used in the evaluation of the expected S_0 and S_m . As an example we mention the case of the form factor, which depends on the nuclear radius and on the thickness parameter for the nuclear surface [19]. We have verified e.g. that varying their values with respect to the standard ones of 20%, the locations of the minima will move toward slightly larger M_w and toward lower $\xi\sigma_p$, while the calculated S_m integrated e.g. in the 2–6 keV energy interval, discussed above, will increase of about 15%.

6 CONCLUSIONS

The data collected over four yearly cycles (total statistics of 57986 kg·day) favour at 4σ C.L. the presence of a yearly modulation in the low energy experimental rate measured deep underground at the Gran Sasso National Laboratory by the $\simeq 100$ kg highly radiopure NaI(Tl) DAMA set-up. Here this effect has been further investigated in terms of

Table 2: Comparison of the residuals in the cumulative 2 – 6 keV energy interval (given as an example in fig. 2) with the values expected when considering the M_w and $\xi\sigma_p$ values of the minima obtained – under standard assumptions – by the cumulative analysis either considering (b) or not (a) the constraint from DAMA/NaI-0. As one can see in these cases, a good agreement is present for DAMA/NaI-1, DAMA/NaI-2 and DAMA/NaI-4, while it is poorer for DAMA/NaI-3 owing to its first two points. The fluctuation of these two residual points is present there in only one of the involved energy bins (obviously in statistics the tails can also play some role). In fact, if, e.g., the 2–5 keV (where most of the signal is expected) residuals would be indeed considered, the $\chi^2/d.o.f.$ values (when taking into account all the residuals over the four yearly cycles) would be 11.5/20 (93% probability) and 12.3/20 (91% probability), respectively. This clearly shows the relevance of performing a complete analysis approach able to properly take into account all the features of the time and energy differential distribution of the events, giving also a C.L. which accounts for the whole behaviour, as it is the standard maximum likelihood method we use.

	$\chi^2/d.o.f.$ (probability)	
	case a)	case b)
DAMA/NaI-1	1.7/2 (43%)	2.1/2 (35%)
DAMA/NaI-2	6.8/5 (23%)	7.7/5 (17%)
DAMA/NaI-3	14.4/7 (4.5%)	15.4/7 (3.2%)
without first 2 points	4.9/5 (43%)	5.3/5 (38%)
DAMA/NaI-4	6.1/6 (42%)	6.5/6 (37%)
DAMA/NaI-1 to 4	29.0/20 (9%)	31.6/20 (4.7%)
without the first 2 points of DAMA/NaI-3	19.5/18 (36%)	21.6/18 (25%)

possible relic neutralinos; the 3σ C.L. allowed contours have been given.

The experiment is continuously running and an upgrading of the electronics has been prepared to verify further peculiarities of the effect to deeply investigate its nature. In incoming years the exposed mass will be increased up to 250 kg.

References

- [1] R. Bernabei et al., *Il Nuovo Cim.* **A112** (1999), 545.
- [2] R. Bernabei et al., *Phys. Lett.* **B389** (1996), 757.
- [3] R. Bernabei et al., *Phys. Lett.* **B408** (1997), 439.
- [4] R. Bernabei et al., *Phys. Lett.* **B424** (1998), 195.
- [5] R. Bernabei et al., *Phys. Lett.* **B450** (1999), 448.

- [6] R. Bernabei et al., in the volume "3K-Cosmology", AIP pub. (1999), 65.
- [7] P. Belli et al., hep-ph/9903501 and *Phys. Rev.* **D61** (2000), 023512.
- [8] P. Belli et al., *Phys. Lett.* **B460** (1999), 236.
- [9] P. Belli et al., *Phys. Rev.* **C60** (1999), 065501.
- [10] R. Bernabei et al., *Phys. Rev. Lett.* **83** (1999), 4918.
- [11] R. Bernabei et al., ROM2F/99/26 to appear in *Il Nuovo Cim.* **A112** (1999).
- [12] K. A. Drukier, et al., *Phys. Rev.* **D33** (1986), 3495.
- [13] K. Freese et al., *Phys. Rev.* **D37** (1988), 3388.
- [14] A. Bottino et al., *Phys. Lett.* **B423** (1998),109; *Phys. Rev.* **D59** (1999), 095004; *Phys. Rev.* **D59** (1999), 095003; *Astrop. Phys.* **10** (1999), 203; hep-ph/9909228 to appear in *Astrop. Phys.*
- [15] R. W. Arnowitt and P. Nath, *Phys. Rev.* **D60** (1999), 044002.
- [16] D. Fargion et al., *Pis'ma Zh. Eksp. Teor. Fiz.* **68**, (JETP Lett. **68**, 685) (1998); to appear on *Astrop. Phys.*
- [17] I. R. Barabanov et al., *Nucl. Phys.* **B546** (1999), 19.
- [18] R. Bernabei, in the volume *Proceed. of the 8-th Int. Workshop on Neutrino Telescopes*, edited by M. Baldo-Ceolin, Papergraf pub., vol. II (1999), 239.
- [19] R.H.Helm, *Phys. Rev.* **104** (1956), 1466.
- [20] M. Ambrosio et al., *Astrop. Phys.* **7** (1997), 109.
- [21] Particle Data Group: Review of Particle Physics, *Eur. Phys. J. C3* (1998), 1.
- [22] P.J.T. Leonard and S. Tremaine, *Astrophys. J.* **353** (1990), 486; C.S. Kochanek, *Astrophys. J.* **457** (1996), 228; K.M. Cudworth, *Astron. J.* **99** (1990), 590.
- [23] K. Hikasa et al., *Phys. Rev.* **D45**, III 38 (1992).
- [24] G. J. Feldman and R. D. Cousins, *Phys. Rev.* **D57** (1998), 3873.